



PERGAMON

Applied Geochemistry 16 (2001) 1499–1512

---

---

**Applied  
Geochemistry**

---

---

www.elsevier.com/locate/apgeochem

# Oxidative dissolution of metacinnabar ( $\beta$ -HgS) by dissolved oxygen

Mark O. Barnett<sup>a,b,\*</sup>, Ralph R. Turner<sup>a</sup>, Philip C. Singer<sup>b</sup><sup>a</sup>*Environmental Sciences Division, Oak Ridge National Laboratory, Oak Ridge, TN, 37831-6038, USA*<sup>b</sup>*Environmental Sciences and Engineering, University of North Carolina, Chapel Hill, NC, 27599-7400, USA*

Received 1 February 2000; accepted 25 August 2000

Editorial handling by J.S. Herman

---

## Abstract

The oxidative dissolution rate of metacinnabar by dissolved O<sub>2</sub> was measured at pH ~5 in batch and column reactors. In the batch reactors, the dissolution rate varied from 3.15 ( $\pm$ 0.40) to 5.87 ( $\pm$ 0.39)  $\times 10^{-2}$   $\mu\text{mol}/\text{m}^2/\text{day}$  (I=0.01 M, 23°C) and increased with stirring speed, a characteristic normally associated with a transport-controlled reaction. However, theoretical calculations, a measured activation energy of 77 ( $\pm$ 8) kJ/mol (I=0.01 M), and the mineral dissolution literature indicate reaction rates this slow are unlikely to be transport controlled. This phenomenon was attributed to the tendency of the hydrophobic source powder to aggregate and minimize the effective outer surface area. However, in a column experiment, the steady-state dissolution rate ranged from 1.34 ( $\pm$ 0.11) to 2.27 ( $\pm$ 0.11)  $\times 10^{-2}$   $\mu\text{mol}/\text{m}^2/\text{day}$  (I=0.01 M, 23°C) and was also influenced by flow rate, suggesting hydrodynamic conditions may influence weathering rates observed in the field. The rate of Hg release to solution, under a range of hydrogeochemical conditions that more closely approximated those in the subsurface, was 1 to 3 orders of magnitude lower than the dissolution rate due to the adsorption of released Hg(II) to the metacinnabar surface. The measured dissolution rates under all conditions were slow compared to the dissolution rates of minerals typically considered stable in the environment, and the adsorption of Hg(II) to the metacinnabar surface further lowered the Hg release rate. © 2001 Elsevier Science Ltd. All rights reserved.

---

## 1. Introduction

Mercury pollution is a wide-spread problem. Increased anthropogenic atmospheric Hg emissions since the industrial revolution have led to an increase in global Hg transport and elevated concentrations in water and fish, even in remote regions (Fitzgerald et al., 1998). Sulfur is an important element in the Hg cycle, as red mercuric sulfide, cinnabar ( $\alpha$ -HgS), is the principal ore of Hg (Adriano, 1986). The formation of HgS in sulfidic waters, sediments, and soils has been postulated as one of the largest sinks for Hg in the environment

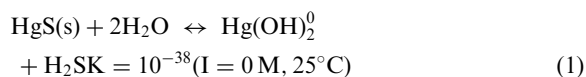
(Stein et al., 1996). Hypolimnetic lake waters, for example, may be over-saturated with respect to HgS which may control Hg solubility (Hurley et al., 1994; Wang and Driscoll, 1995). Mercuric sulfide may also form in marine sediments (Sakamoto et al., 1995) and in soils (Lechler et al., 1997). Satake et al. (1990) have shown that small crystals of black HgS, metacinnabar ( $\beta$ -HgS), form in aquatic plants, and that the subsequent death and decay of the plants would result in the introduction of HgS to the water column. Barnett et al. (1997) have shown that small crystals of metacinnabar have formed in a Hg-contaminated floodplain soil consequent to SO<sub>4</sub><sup>2-</sup> reduction in the soils. Although trigonal cinnabar is stable relative to cubic metacinnabar at temperatures below 350°C, impurities such as Fe which are common in the ambient environment can stabilize the metacinnabar crystal structure (Tauson and Akimov, 1997).

---

\* Corresponding author at current address: 208 Harbert Engineering Center, Department of Civil Engineering, Auburn University, AL 36849, USA. Fax: +1-334-844-6290.

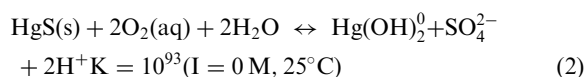
E-mail address: barnettm@eng.auburn.edu (M.O. Barnett).

Mercuric sulfide is very insoluble and is much less leachable and volatile from soils than other pure solid Hg forms (Willett et al., 1992). Because of its low solubility, it has been suggested that the formation of HgS in the environment, either by natural means (Krabbenhoft and Babiarz, 1992) or as a result of engineered processes (Kaiser and Tolg, 1980), may limit Hg cycling through the biosphere. Despite its potential to serve as either a natural or man-made sink for Hg, the long-term stability of metacinnabar will impact its efficacy as a Hg repository. Because of its extreme insolubility, the weathering of HgS by simple dissolution



is thermodynamically limited as the equilibrium constant for reaction (1) indicates. An exception to this statement may occur in environments with high dissolved sulfide concentrations which form strong complexes with Hg(II) and will promote its dissolution (Paquette and Helz, 1997).

However, HgS, owing to the presence of reduced S, is thermodynamically unstable in the presence of dissolved O<sub>2</sub> or other oxidants common in the environment. The equilibrium constant for the oxidative dissolution of HgS by dissolved O<sub>2</sub>



given by reaction (2) is much larger than the one in reaction (1). Therefore, dissolution will have a much larger thermodynamic driving force in the presence of any dissolved O<sub>2</sub>. Weathering by oxidative dissolution would be of concern whenever HgS was exposed to oxidizing conditions (e.g. in disturbed sediments, lowering of the water table in a shallow aquifer, etc.). To the extent HgS is kinetically resistant to oxidation, once formed, it may remain stable in the environment, even under oxidizing conditions. There is very little published quantitative information on the oxidation rate of HgS. However, its persistence in oxic environments near mines suggests it weathers slowly under aerobic conditions (Azzaria and Aftabi, 1991; Plouffe, 1997).

The purpose of this paper is to describe the results of an investigation into the stability of metacinnabar with respect to oxidative dissolution by dissolved O<sub>2</sub> in the subsurface. This study focused on metacinnabar to determine the influence of oxidative dissolution in Hg cycling in contaminated environments. Authigenic metacinnabar has been identified in Hg-contaminated soil (Barnett et al., 1997) and is the most likely authigenic polymorph of HgS in the subsurface at Hg-contaminated

sites due to the presence of impurities (e.g. Fe) that stabilize its crystal structure (Tauson and Akimov, 1997). Dissolution rates were measured in both batch and column experiments to examine the influence of hydrodynamics on the dissolution rate. Because the rate of release of Hg was much lower than the dissolution rate, the adsorption of Hg(II) to metacinnabar was also investigated. In addition, the export of Hg (i.e., the effective weathering rate in terms of Hg release) from columns containing metacinnabar were measured under conditions designed to mimic those in the subsurface. These results are important in assessing the potential role of metacinnabar as a Hg repository in the subsurface.

## 2. Experimental and analytical methods

### 2.1. Experimental methods

Reagent-grade metacinnabar (Aldrich Chemical Company, Hg(II) sulfide, black powder, Lot. No. 04609TZ) was used in this study because a metacinnabar ore of reasonable purity could not be located. Several subsamples of the material were analyzed by X-ray diffraction, and metacinnabar was the only crystalline material identified. Subsamples were also analyzed with a scanning electron microscope (SEM), which revealed the material consisted of aggregates comprised of micron- and submicron-sized crystals. The surface area was measured as  $0.98 \pm 0.07 \text{ m}^2/\text{g}$  (all uncertainties are shown as  $\pm$  the sample standard deviation unless otherwise noted) by N<sub>2</sub> BET adsorption. Surface area measurements of different nominal particle sizes were not significantly different, indicating the surface area was controlled by the individual crystal size and not the aggregate particle size.

Oxidation rates were measured in both batch and column experiments. Batch experiments were conducted in 1 l Teflon containers that were wrapped in Al foil to prevent light from potentially increasing the reaction rate (Okouchi and Sasaki, 1983). Humidified Grade A compressed air was bubbled through a Teflon diffuser into a suspension of metacinnabar adjusted to a constant ionic strength with 0.01 M NaNO<sub>3</sub>. The reactor was stirred with a magnetic stirrer and a Teflon-coated stir bar that was suspended a few cm off the reactor bottom by a Teflon-coated frame to minimize grinding of the particles during the experiment. The stirring speed was measured with a strobe light and controlled by adjusting the voltage to the stirrer. The temperature in the batch reactors was 23.0 ( $\pm 0.5$  range) °C. In some experiments, Au-coated sand traps were placed on the air outlet line and subsequently analyzed for Hg to determine if Hg was being volatilized from the reactors.

Total S (measured as SO<sub>4</sub><sup>2-</sup>) was selected as the primary reaction progress variable as shown in reaction

(2), although  $H^+$  production was also monitored as a secondary reaction progress variable. The metacinnabar was washed 3 times with distilled water and then dried in a vacuum-evacuated desiccator prior to use. The use of more aggressive cleaning procedures (e.g. alcohol, acids, bases) caused the production of elemental S and colloidal metacinnabar and other experimental problems. Periodically the pH was monitored in the reactor and adjusted with NaOH as needed to maintain a pH of  $4.7 \pm 0.1$ , which was selected because the pH could be maintained at a relatively constant value without the use of buffers, which might have influenced the reaction rate. The effect of pH on the Hg release rate was subsequently examined in column experiments. Small samples were taken periodically during the experiment with a glass syringe through a Teflon sampling tube. The samples were filtered with either a 0.2 or 0.45  $\mu m$  syringe filter and analyzed for  $SO_4^{2-}$ . Several experiments were conducted under sterile conditions in a Bioguard hood, and there was no significant difference between the reaction rates measured under sterile and non-sterile conditions, suggesting that microorganisms did not influence the reaction rates in these experiments. At the end of some experiments, the remaining solution was decanted and filtered with a 0.2 or 0.45  $\mu m$  filter and analyzed for total Hg. Samples analyzed before and after oxidation with  $H_2O_2$  (see below) indicated colloidal HgS was not passing through the filters.

Column experiments were used to measure both the dissolution rate and the Hg release rate under physical and chemical conditions closer to those found in the subsurface (e.g. in porous media, in the presence of natural organic matter, etc.). Two sets of column experiments (Table 1) were conducted in 1 cm diameter adjustable-length glass chromatography columns with small-diameter inlet and outlet Teflon tubing and fittings to minimize dead volume. The columns were packed with metacinnabar and acid-washed silica sand

and wrapped in Al foil to minimize light entering the column. Column hydrodynamics were quantified by measuring the concentration breakthrough of an inorganic tracer ( $Cl^-$  or  $Br^-$ ).

Column 1 was designed to measure the dissolution rate and thus utilized a high metacinnabar concentration and a lower flow rate (see Table 1) to produce  $SO_4^{2-}$  concentrations high enough to be measured, from which the dissolution rate was calculated. An air-saturated solution of 0.01 M  $NaNO_3$  was pumped up through the column with a volumetric microinfusion pump at a specific discharge of 1.27 cm/h. Air-saturated solutions were prepared by bubbling the solutions with air until the dissolved  $O_2$  level was constant at the theoretical saturation level for that temperature. Samples were collected over approximately one pore volume and analyzed for total dissolved Hg,  $SO_4^{2-}$ , and pH. After approximately 14 days, the inlet solution was switched from air-saturated 0.01 M  $NaNO_3$  to 0.01 M NaCl to investigate the effects of increasing the complexing capacity for Hg(II) on Hg transport from the column. Finally, after 34 days the specific discharge was decreased to 0.63 cm/h to measure the effect of a decreased flow rate on the oxidation rate.

Column 2 was designed to measure the Hg release rate during weathering and thus used a lower HgS concentration and a higher flow rate than Column 1. The column was packed with an HgS concentration of 2000 mg/kg to replicate the conditions of East Fork Poplar Creek (EFPC), a Hg-contaminated site where metacinnabar has formed due to  $SO_4^{2-}$  reduction in the soils (Barnett et al., 1997). Three solutions were used to reflect a range of chemical compositions that may be encountered in the subsurface: 0.01 M NaCl with pH adjusted with  $HNO_3$  or NaOH from 5 to 9 to examine the effect of pH on the Hg release rate, and two natural waters (Table 2), a low-dissolved organic C (DOC) natural surface water from White Oak Creek (WOC) in

Table 1  
Summary description of column experiments performed in this study

Experiment	Column	$q$ (cm/h)	Eluent	Dissolution rate ( $\mu mol/m^2/day$ )	Hg release rate ( $\mu mol/m^2/day$ )
A	1 <sup>a</sup>	1.27	0.01 M $NaNO_3$	$2.27 \times 10^{-2}$	< Detection limit
B	1 <sup>a</sup>	1.27	0.01 M NaCl	$1.64 \times 10^{-2}$	< Detection limit
C	1 <sup>a</sup>	0.635	0.01 M NaCl	$1.34 \times 10^{-2}$	< Detection limit
D	2 <sup>b</sup>	12.7	0.01 M NaCl pH 5–9	< Detection limit	$6.97 \times 10^{-5}$ – $1.42 \times 10^{-3}$
E	2 <sup>b</sup>	12.7	WOC water <sup>c</sup>	< Detection limit	$1.97 \times 10^{-3}$ – $3.62 \times 10^{-3}$
F	2 <sup>b</sup>	12.7	EVG water <sup>c</sup>	< Detection limit	$2.71 \times 10^{-3}$ – $5.02 \times 10^{-3}$
G	2 <sup>b</sup>	1.27	EVG water	< Detection limit	$2.67 \times 10^{-5}$ – $2.45 \times 10^{-4}$

<sup>a</sup> Column 1: volumetric water content,  $\theta$ , 0.443  $cm^3/cm^3$ ; bulk density,  $\rho_b$ , 1.56  $g/cm^3$ ; HgS content 100,000 mg/kg; column Peclet number,  $N_{Pe}$ , 875 ( $q = 1.27$  cm/h).

<sup>b</sup> Column 2: volumetric water content,  $\theta$ , 0.444  $cm^3/cm^3$ ; bulk density,  $\rho_b$ , 1.48  $g/cm^3$ ; HgS content 1980 mg/kg; column Peclet number,  $N_{Pe}$ , 1130 ( $q = 12.7$  cm/h).

<sup>c</sup> WOC, White Oak Creek; EVG, Everglades.

Table 2  
Surface water composition (all concentrations in mol/l unless noted otherwise)

Component	White Oak Creek	Everglades
Ca	$4.26 \times 10^{-4}$	$1.83 \times 10^{-3}$
K	$< 2.5 \times 10^{-5}$	$2.51 \times 10^{-4}$
Mg	$1.60 \times 10^{-4}$	$6.92 \times 10^{-4}$
Na	$2.52 \times 10^{-5}$	$2.71 \times 10^{-3}$
Cl	$3.02 \times 10^{-5}$	$1.79 \times 10^{-3}$
NO <sub>3</sub>	$8.87 \times 10^{-6}$	$4.57 \times 10^{-4}$
SO <sub>4</sub>	$5.94 \times 10^{-5}$	$2.99 \times 10^{-4}$
Si	$1.01 \times 10^{-4}$	$2.29 \times 10^{-4}$
Hg	$< 5.0 \times 10^{-11}$	$< 5.0 \times 10^{-11}$
Alkalinity (eq/l)	$1.38 \times 10^{-3}$	$3.621 \times 10^{-3}$
pH	7.67	7.46
DOC (mg/l)	2.50	30.5

East Tennessee and a high-DOC natural surface water from the Everglades (EVG). Column effluent samples were analyzed for total dissolved Hg, SO<sub>4</sub><sup>2-</sup>, and pH.

Mercury(II)-metacinnabar adsorption was studied in batch experiments conducted in 250 ml Teflon bottles using the bottle-point technique. From 0.15 to 1.00 g of metacinnabar were added to each bottle, which was then filled with pH 4.0, 0.01 M NaCl containing approximately 500 µg/l of Hg(II) diluted from a commercial Hg(II) standard. The bottles were placed on a shaker table for 48 h at room temperature ( $23 \pm 1.5^\circ\text{C}$ ), then removed and filtered with a 0.2 µm filter. Replicate samples allowed to equilibrate for several additional days did not show a significantly greater degree of adsorption. The filtrate was analyzed for total Hg, and the Hg(II) assumed to be adsorbed to the metacinnabar (Burkstaller et al., 1975) was calculated from the difference between the initial and final Hg(II) concentrations.

A blank containing no metacinnabar was run to verify that there were no losses of Hg due to volatilization or adsorption, either to the filter or to the container walls, over the duration of the experiment. Another blank was run with metacinnabar under identical solution conditions but without any added Hg(II). The equilibrium Hg concentration in the metacinnabar-containing blank was 25 pM (5 ng/l), 5 orders of magnitude below the added Hg concentration and lower than the Hg concentration in a third blank (45 pM, 9 ng/l) without either metacinnabar or added Hg(II). Mercury in otherwise "Hg-free" solutions is due to the presence of Hg in small amounts in chemicals used to adjust the ionic strength, pH, etc. The concentration of any readily-labile Hg(II) adsorbed to the metacinnabar prior to the start of the experiment was measured by extracting the metacinnabar with 1 M HCl for 1 h. Only 0.026 ( $\pm 0.003$ ) µg of Hg/g of metacinnabar was extracted during this procedure. The concentration of Hg adsorbed to the metacinnabar prior to the start of the

experiment was thus assumed negligible compared to the amount of Hg(II) added during the adsorption experiments and was not considered further in the analysis.

## 2.2. Analytical methods

Samples to be analyzed for SO<sub>4</sub><sup>2-</sup>, Cl<sup>-</sup>, Br<sup>-</sup>, and NO<sub>3</sub><sup>-</sup> were refrigerated and analyzed by ion chromatography similar to ASTM Method D 4327 (ASTM, 1991). At least 10% of the samples analyzed for SO<sub>4</sub><sup>2-</sup> were analyzed again after oxidation by H<sub>2</sub>O<sub>2</sub> (Hoffman, 1977) to ensure that all the dissolved S was present as SO<sub>4</sub><sup>2-</sup>. There was no significant difference between SO<sub>4</sub><sup>2-</sup> concentrations measured before and after oxidation with H<sub>2</sub>O<sub>2</sub>, and no unknown peaks suggestive of thiosulfate or sulfite were seen in the chromatographs. Samples were analyzed for total Hg by either cold vapor atomic absorption (CVAA) or fluorescence (CVAF) similar to EPA Method 7470 (EPA, 1986) or Method 1631 (EPA, 1995). Dissolved O<sub>2</sub> (DO) measurements were made with a DO meter and probe. Measurements of pH were made with a combination pH electrode and meter. Proton production was calculated from pH measurements and equilibrium relationships using the Güntleberg approximation of the Debye-Hückel theory for activity corrections.

## 3. Results and discussion

### 3.1. Batch oxidation experiments

Fig. 1 shows the results of a typical batch experiment as a plot of total S (measured as SO<sub>4</sub><sup>2-</sup>) produced versus time. The data typically exhibited a period of initially rapid dissolution lasting for less than a day (not shown). An initially rapid period of dissolution is a commonly encountered phenomenon in mineral dissolution experiments (Lasaga, 1984; Drever, 1988), and is typically due to the rapid dissolution of fine particles or oxidation products formed during sample preparation, which is difficult if not impossible to avoid in sulfide mineral oxidation experiments (Moses et al., 1987; Nicholson et al., 1988). After this initial period, linear (with time) dissolution occurred until the experiment ended or experimental conditions changed (in Fig. 1, the stirring rate was decreased after 5 days as discussed below). The dissolution rate was estimated for each experiment via linear regression from the slope of the steady-state, linear portion of the data. Experiments typically lasted 7 days, and at least 5 data points were used to estimate the slope in all experiments. This portion of the data was well fit by linear regression, as the coefficient of determination ( $r^2$ ) in most experiments was  $> 0.99$ . From the volumetric rate, specific reaction rates were calculated

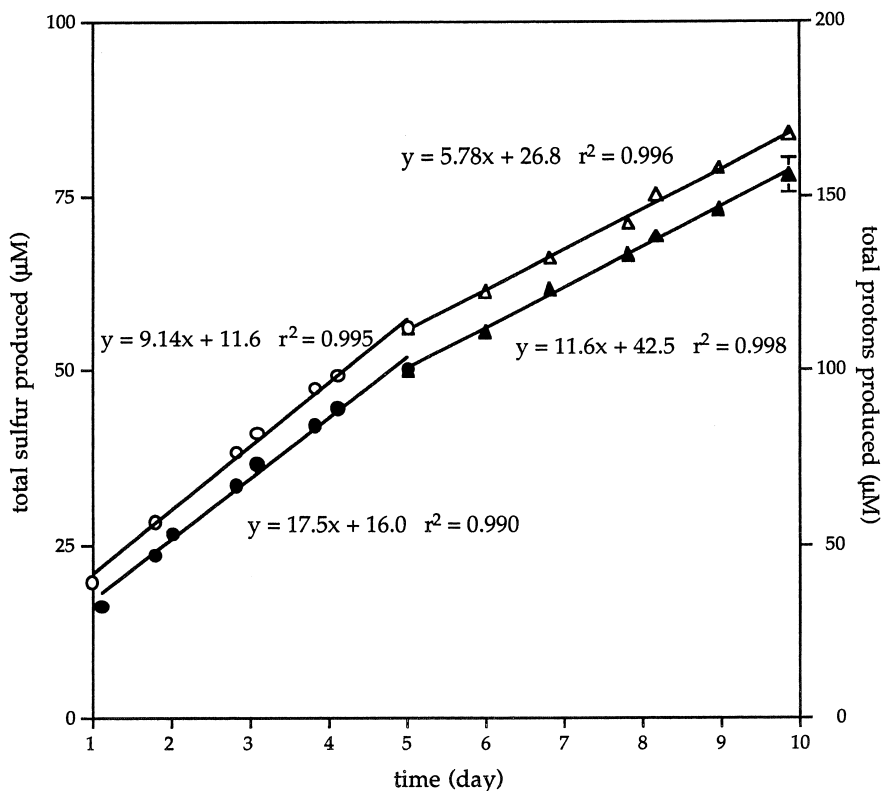


Fig. 1. Results of a batch oxidation rate experiment ( $I = 0.01 \text{ M}$ ,  $T = 23^\circ\text{C}$ ). The stirring speed was slowed from 220 to 125 rpm after 5 days. Open circles show the total S (measured as  $\text{SO}_4^{2-}$ ) produced versus time at 220 rpm and open triangles show the total S produced at 125 rpm. Error bars for the  $\text{SO}_4^{2-}$  measurements are smaller than the data points. Filled circles show the total  $\text{H}^+$  produced versus time at 220 rpm and filled triangles show the total  $\text{H}^+$  produced at 125 rpm. Error bars on one point show the estimated error based on a pH measurement error of  $\pm 0.05$  units. Lines and equations show the linear regression fits of the data. The volumetric reaction rates were determined from the slopes of the lines and converted to specific reaction rates from solids concentration and surface area. Note the scale for  $\text{H}^+$  produced is twice the scale for the total S produced to match the proposed stoichiometry. Rates as measured by total S and  $\text{H}^+$  production decreased when the stirring speed was decreased.

using the solid/solution ratio and the measured specific surface area.

The effect of stirring speed on the reaction rates was investigated by measuring the reaction rates at stirring bar speeds ranging from 0 to 220 rpm (at 0 rpm the reactor was stirred briefly just prior to sampling to ensure the solution was homogeneous). It was originally hypothesized that the dissolution rate would be independent of stirring speed. Stirring speed dependence is usually indicative of mass-transfer controlled dissolution. The dissolution rate of relatively insoluble ( $< 1 \mu\text{mol/l}$ ) minerals such as metacinnabar is typically controlled by surface reactions rather than mass transfer limitations (Appelo and Postma, 1993). However, as shown in Table 3, there was a small (the uncertainty in mineral weathering rates measured in the laboratory is typically about an order of magnitude (Brezonik, 1994)) but significant ( $P < 0.05$ ) increase in reaction rate with stirring speed. The effect of stirring speed on dissolution rate can be clearly seen in Fig. 1, where a stirring speed

decrease from 220 rpm to 125 after 5 days was accompanied by a decrease in the  $\text{SO}_4^{2-}$  and  $\text{H}^+$  production rate.

The finding of an apparent mass-transfer limitation (i.e. stirring-speed dependence) in these experiments was surprising. The slowest form of mass-transfer-limited mineral dissolution would occur in a quiescent, purely diffusion-controlled system. The dissolution rate of particles in such a system is given by (Nielsen, 1964)

$$R_{\text{specific}} = \frac{D}{r}(C_S - C_B) \quad (3)$$

where  $D$  is the solute diffusion coefficient ( $\text{length}^2/\text{time}$ ),  $r$  is the particle radius ( $\text{length}$ ) and  $C_S$  and  $C_B$  are the equilibrium and bulk concentration ( $\text{mol}/\text{length}^3$ ) of the diffusing solute respectively. If the dissolution rate is diffusion-controlled, the only rate-limiting step would be the transport of the sole aqueous-phase reactant (dissolved  $\text{O}_2$ ) from the bulk solution to the solid/water

Table 3  
Reaction rates as a function of stirring speed (pH 4.7, I = 0.01 M, 23°C)

Stirring rate (rpm)	Rate ×100 (μmol/m <sup>2</sup> /day)	Average ×100 (μmol/m <sup>2</sup> /day)	Standard deviation ×100 (μmol/m <sup>2</sup> /day)	Coefficient of variation (%)
0	2.68 2.96 3.44 3.51	3.15	0.40	12.6
125	4.01 3.85 3.86 3.98 4.17 3.98	3.98	0.12	2.9
175	4.56 4.29 3.79 5.17 4.62 4.09 4.29	4.40	0.44	10.0
220	6.30 5.53 5.78	5.87	0.39	6.7

interface. The concentration of dissolved O<sub>2</sub> in the bulk solution was maintained at a constant level of 0.26 mM (8.30 mg/l) by bubbling air through the reactor, and, if the transport of dissolved O<sub>2</sub> was rate-limiting, the concentration at the solid water interface would be zero. Using these values, a particle radius of 0.4 μm (the equivalent spherical radius calculated from surface area measurements), a diffusion coefficient for dissolved O<sub>2</sub> of  $2.35 \times 10^{-5}$  cm<sup>2</sup>/s (Thibodeaux, 1996) and Eq. (3), a theoretical mass-transfer-limited dissolution rate of 65 mol HgS/m<sup>2</sup>/day was calculated. Since the calculated rate is many orders of magnitude faster than the rates reported in Table 3, mass-transfer cannot be limiting the dissolution rate. These predictions are typically confirmed experimentally, though rate data as a function of stirring speed are rarely presented. McKibben and Barnes (1986), for example, measured oxidative dissolution rates of pyrite in stirred batch reactors that were orders of magnitude higher than those shown in Table 3 and reported that the rates were independent of the stirring speed.

To further investigate the unexpected mass-transfer dependency observed in the batch experiments (Table 3), the activation energy was measured by repeating the experiments at 15 and 19°C while maintaining a constant stirring rate of 175 rpm. This relatively small temperature change increased the dissolved O<sub>2</sub> concentration by <10%, which minimized the accom-

panying potential effects on reaction rate. The results are shown in the form of an Arrhenius plot in Fig. 2. An activation energy of 77 (±8) kJ/mol (I = 0.01 M) was estimated from the slope of the line in Fig. 2.

The measured activation energy is lower than the range required for the breaking of bonds in crystals (160–400 kJ/mol) but is within the range of values reported for pyrite oxidation by dissolved O<sub>2</sub> (Nicholson et al., 1988) and within the relatively narrow range (40–80 kJ/mol) reported for dissolution of silicate minerals (Lasaga, 1984). However, it is much larger than activation energies measured for diffusion (i.e. transport) controlled reactions, which typically have activation energies on the order of about 20 kJ/mol (Drever, 1988). Thus, the results shown in Table 3 and Fig. 2 are inconsistent; the reaction rate appears to be dependent on stirring rate, suggesting that the rate is transport-limited, but the activation energy of the rate-determining step is not consistent with diffusional control.

It is possible that the reaction is in a mixed control regime, i.e. there is some degree of control by both chemical and diffusional processes. It is also possible that some other experimental artifact is mimicking transport control. Metacinnabar is hydrophobic due to the non-ionic nature of the Hg–S bond, and the powder tended to clump together, apparently minimizing the outer wetted surface area. Increasing the stirring rate visibly

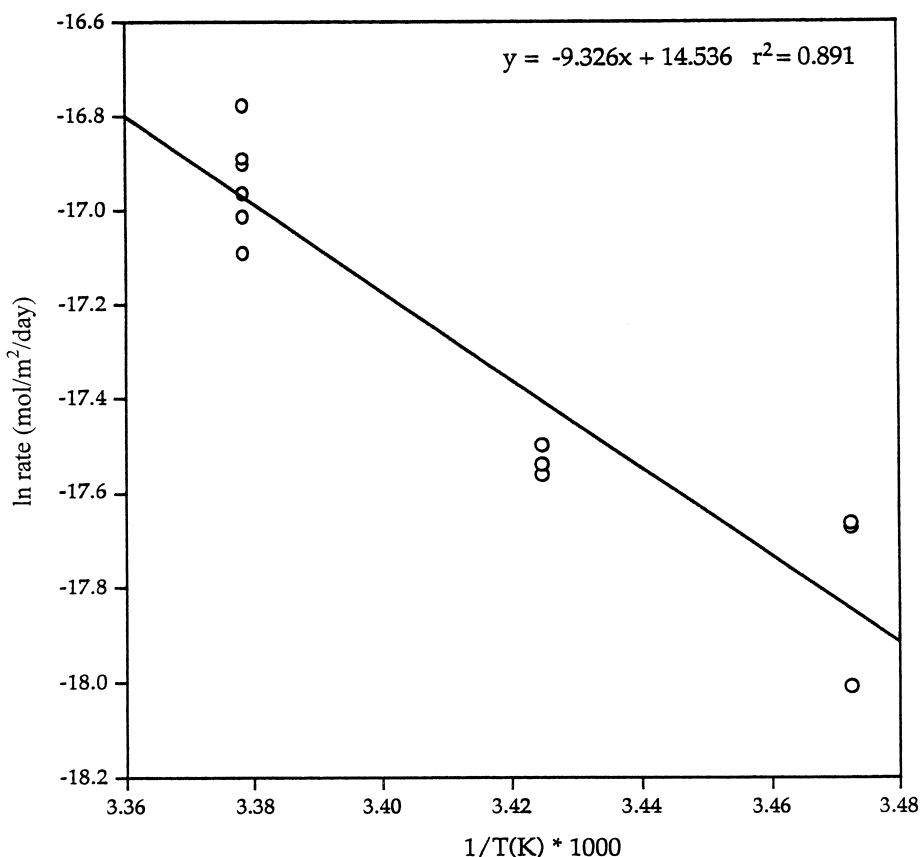


Fig. 2. Arrhenius plot of dissolution rate ( $I=0.01$  M,  $23^\circ\text{C}$ ). Stirring speed was constant at 175 rpm.

decreased the size of the individual powder clumps. Thus it is possible that increasing the stirring rate could increase the reaction rate simply by increasing the effective surface area, mimicking transport control. There was no evidence of a true surface area change over the course of the experiments; dry surface areas measured by BET adsorption before and after the experiments did not change significantly. In addition, the rate measured during the course of an experiment could be decreased by lowering the stirring speed as shown in Fig. 1, indicating rapid stirring did not induce a permanent effect on the reaction rate as would be expected from a change in true surface area. These results, although surprising, are consistent with the recent data of Ravichandran et al. (1998) who found that the DOC-enhanced dissolution of cinnabar was strongly dependent on the degree of mixing. As a result of this unexpected observation, additional dissolution rate experiments were conducted in packed columns (below) under hydrodynamic conditions that were closer to those encountered in the sub-surface.

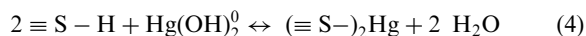
In all the batch experiments in which the final solution was analyzed for total Hg by CVAA spectroscopy, the total Hg concentration was  $< 1$  nM ( $< 0.2$   $\mu\text{g/l}$ ), the

minimum detectable concentration. Analyses of the Au traps on the air outlet of some experiments indicated Hg was not being transported from the reactor in the exhaust stream. However, if the metacinnabar was oxidized at the rates shown in Table 3 and described by reaction (2), a Hg sink must exist within the reactor. Since the reactor was of all Teflon-construction, which minimizes Hg adsorption, the only remaining sink was the metacinnabar itself. Burkstaller et al. (1975) studied the oxidation of cinnabar by Fe(III) in acid mine drainage and reported that the Hg release rate was much lower than the dissolution rate (measured by the reduction rate of Fe(III)), concluding that the Hg released during oxidative dissolution was being sorbed to the cinnabar surface.

Further insight into the fate of Hg(II) generated during oxidation can be obtained by examining the  $\text{H}^+$  production rate. Fig. 1 also shows the cumulative  $\text{H}^+$  production versus time which is consistent with two mol of  $\text{H}^+$  for every mol of  $\text{SO}_4^{2-}$  produced. This stoichiometry was observed consistently in the batch reactors regardless of stirring speed and corresponds to the oxidative dissolution reaction shown in reaction (2). Reaction (2), however, can not be correct as written due to

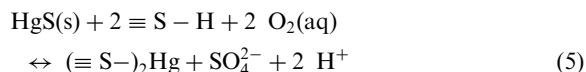
the lack of any observed dissolved Hg production. For the reaction to be correct, the adsorption of Hg(II) to the metacinnabar surface must be included in the reaction while preserving the observed  $H^+$  and  $SO_4^{2-}$  stoichiometry.

Using a surface complexation framework (Stumm, 1992), the adsorption of Hg(II) to the metacinnabar surface can be described as the interaction of the chalcophile Hg(II) with mineral surface sulfhydryl groups (represented by  $\equiv S-H$ ) by the following reaction



Reaction (4) was written as a surface complexation reaction, which is consistent with the current surface complexation theory for mineral sulfides (Ronngren et al., 1991), and which has the proposed adsorbed Hg(II) species in two-fold coordination with  $\equiv S-$ , analogous to the predominant aqueous Hg(II)-S(-II) complexes (Paquette and Helz, 1997).

The addition of reactions (2) and (4) gives



as the oxidative dissolution reaction. In the absence of direct spectroscopic evidence, it is not possible to unequivocally identify specific surface species nor even the mechanism by which the Hg(II) is retained on the solid surface. However, reaction (5) is consistent with the  $SO_4^{2-}$ ,  $H^+$  and Hg(II) production observed in this study in both batch and column experiments as discussed below.

### 3.2. Column oxidation experiments

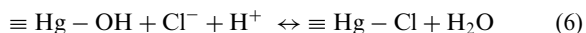
Due to the observation of an apparent unexpected mass transfer effect in the batch experiments, the dissolution rate was also investigated in a packed column to measure the rate under hydrodynamic conditions more representative of those which might be found in the field. In addition, a CVAF was utilized to measure Hg levels in the effluent, greatly lowering the minimum detectable dissolved Hg concentration. The results of column oxidation experiments A–C (Table 1) are shown in Fig. 3. The specific reaction rate at each point was calculated from the  $SO_4^{2-}$  concentration for each point from the stoichiometry of Eq. (1), the flow rate, the total mass of metacinnabar in the column, and the specific surface area of the metacinnabar. The initial eluent was 0.01 M  $NaNO_3$  (Experiment A, Table 1). The  $SO_4^{2-}$  concentration in the effluent decreased rapidly for the first 4 days, and then remained at a relatively constant level over the next 9 days. The steady-state oxidation rate over this time frame (approximately 4–13 days) was  $2.27 (\pm 0.19) \times 10^{-2} \mu\text{mol}/\text{m}^2/\text{day}$  ( $I=0.01 \text{ M}$ ,  $23^\circ\text{C}$ )

which is comparable to the average oxidation rate of  $3.15 (\pm 0.40) \times 10^{-2} \mu\text{mol}/\text{m}^2/\text{day}$  ( $I=0.01 \text{ M}$ ,  $23^\circ\text{C}$ ) in the unstirred batch experiments.

The Hg concentration in the effluent averaged  $40 \pm 20 \text{ pM}$  ( $8 \pm 4 \text{ ng/l}$ ) which was not significantly above the influent concentration of  $26 \pm 4 \text{ pM}$  ( $5.3 \pm 0.8 \text{ ng/l}$ ). Thus the Hg release rate was several orders of magnitude lower on a molar basis than the  $SO_4^{2-}$  production rate. The low Hg release rate compared to the metacinnabar oxidation rate greatly lowers the effective weathering rate (i.e. in terms of Hg release) of metacinnabar. For perspective, the average effluent Hg concentration from the column, which contained 10% metacinnabar by mass, was in the same range as those typically measured in rain and groundwaters, even in areas without local sources of Hg (Krabbenhoft and Babiarz, 1992). In order to investigate the effect of increasing the complexing capacity for Hg(II) on the transport of Hg from the column, the influent was switched from air-saturated 0.01 M  $NaNO_3$  to 0.01 M  $NaCl$  (Experiment B, Table 1) after approximately 14 days (shown with a vertical line in Fig. 3). Although the addition of 0.01 M chloride increased the Hg-complexing capacity by greater than 6 orders of magnitude compared to the hydroxo complex at pH 4.7, the effluent Hg concentration did not significantly change.

The effluent pH from the column ranged from 4.50 to 5.65, for an average of 5.00. Also shown in Fig. 3 is the  $H^+$  produced in each sample. Proton production in the column was calculated from the pH difference between the inlet and outlet concentrations, after activity corrections and a correction for atmospheric  $CO_2$ . This approach assumed the contribution from pure  $H^+$  exchange with the column media was negligible. The close agreement between the  $SO_4^{2-}$  concentration and  $H^+$  production indicates the stoichiometry of Eq. (5) is followed in the column as well.

The only systematic departure from the stoichiometry of reaction (5) is the immediate decrease in  $H^+$  production just after switching from 0.01 M  $NaNO_3$  to 0.01 M  $NaCl$ . The  $H^+$  production decreased (the effluent pH increased to 5.65, the same pH as the air-saturated influent), and then gradually increased again in accordance with the stoichiometry of Eq. (5). The decrease in  $H^+$  production during this phase may be due to the surface complexation of  $Cl^-$  ions, which form important complexes with dissolved Hg(II) at pH 4.7, to Hg(II) surface species (represented by  $\equiv Hg-OH$ ) as shown by reaction (6)



By this proposed mechanism, the observed decrease in  $H^+$  production would be a net decrease, with the  $H^+$  produced by reaction (5) temporarily offset by the  $H^+$  consumption of reaction (6). However, once the

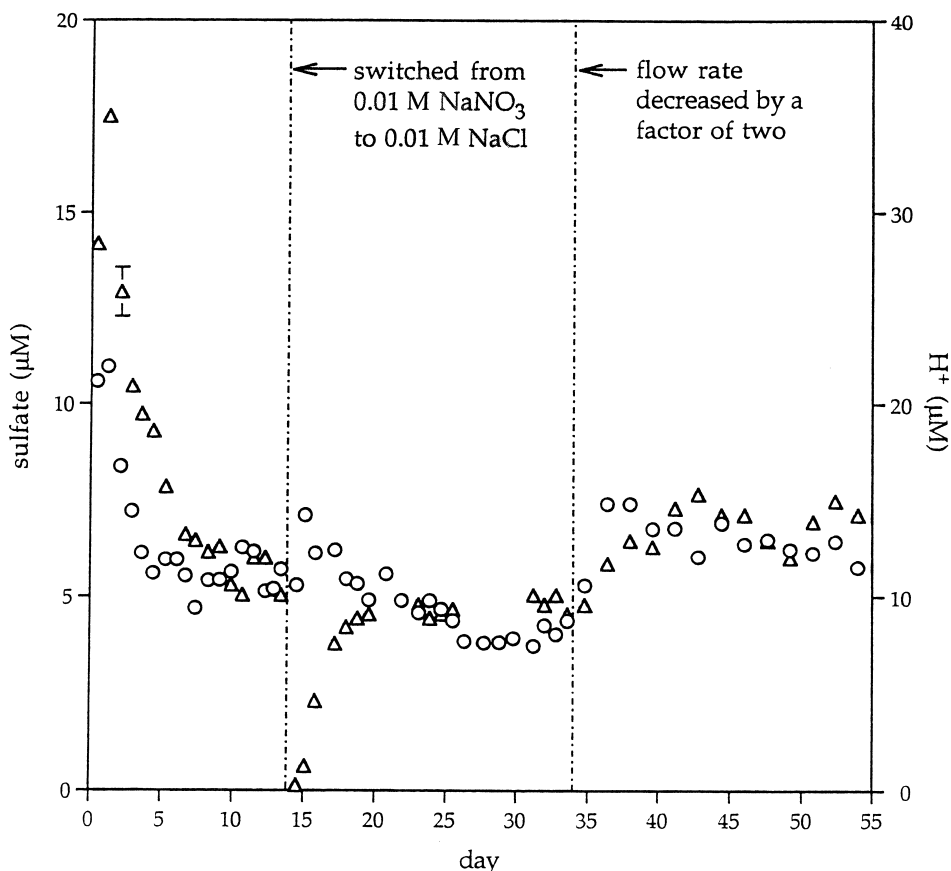


Fig. 3. Sulfate and protons produced in column 1 effluent ( $I=0.01$  M,  $T=23^{\circ}\text{C}$ ). Error bars for the  $\text{SO}_4^{2-}$  measurements (circles) are smaller than the data points. Proton production (triangles) was calculated from pH measurements. The error bar indicates the estimated error associated with an uncertainty in pH measurements of  $\pm 0.05$  units. Note the scale for  $\text{H}^+$  is twice the scale for  $\text{SO}_4^{2-}$ .

Cl-concentration in the column and reaction (6) reached equilibrium, no further  $\text{H}^+$  would be consumed, and the  $\text{H}^+$  production would again revert to that described by reaction (5), which is consistent with the experimental data.

After switching from 0.01 M  $\text{NaNO}_3$  to 0.01 M  $\text{NaCl}$ , the effluent  $\text{SO}_4^{2-}$  concentration increased briefly and then decreased to yield a steady-state oxidation rate of  $1.64 (\pm 0.11) \times 10^{-2} \mu\text{mol}/\text{m}^2/\text{day}$  ( $I=0.01$  M,  $23^{\circ}\text{C}$ ) for approximately 8 days. It is uncertain if the decrease in the steady-state rate after switching from 0.01 M  $\text{NaNO}_3$  to 0.01 M  $\text{NaCl}$  was due to the change in the background electrolyte or simply a general decline in the reaction rate with time previously observed in column dissolution studies. Nicholson et al. (1990) interpreted the decrease in pyrite oxidation rates with time in a packed column as indicating the dissolution rate was controlled by the diffusion of  $\text{O}_2$  through an accumulating Fe oxide product coating on the pyrite surface. By reaction (5), adsorbed  $\text{Hg}(\text{II})$  also accumulates on the surface of metacinnabar during dissolution, potentially

lowering the dissolution rate by blocking reactive surface sites. Theoretical calculations based on the ionic radius of  $\text{Hg}(\text{II})$  and the available surface area indicate that the released Hg would constitute an insignificant fraction (approximately 1%) of the total surface area over the duration of the experiments in this investigation if the Hg adsorbed as a monolayer. However, it is likely that Hg would tend to adsorb to the surface sites of highest energy, which would also be the most active dissolution sites. Therefore, it is not possible to determine which mechanisms are responsible for the decrease in the steady-state reaction rate shown in Fig. 3. Longer-term experiments with larger metacinnabar crystals and a more narrow size distribution, coupled with surface spectroscopic methods, would be helpful in resolving this question.

In order to further investigate the hydrodynamic dependence observed in the batch experiment, the inlet flow rate was decreased by a factor of two (Experiment C, Table 1) after approximately 34 days as shown by the second vertical line in Fig. 3. The  $\text{SO}_4^{2-}$  concentration in

the effluent increased immediately due to the longer hydraulic residence time, but increased by less than a factor of two. The steady-state oxidation rate decreased significantly ( $P < 0.05$ ) from  $1.64 (\pm 0.11)$  to  $1.34 (\pm 0.11) \times 10^{-2} \mu\text{mol}/\text{m}^2/\text{day}$  ( $I = 0.01 \text{ M}$ ,  $23^\circ\text{C}$ ) when the flow rate was decreased by a factor of two. The dissolution rates measured in this study were dependent upon the prevailing hydrodynamic conditions in both batch and column experiments and thus may exhibit the same sort of dependence in the field as well.

In order to provide some perspective on the rates measured above, some dissolution rates for other minerals of interest are shown in Table 4. The oxidation of cinnabar by Fe(III) iron in simulated acid mine drainage (Burkstaller et al., 1975) was one to two orders of magnitude faster than the rates measured in this investigation, as acidic conditions and Fe(III) are known to catalyze sulfide mineral oxidation. The oxidation rate of pyrite (Nicholson et al., 1988) under conditions similar to this study (by dissolved  $\text{O}_2$  at near-neutral pH values) was at least an order of magnitude faster on a per mass basis. Lasaga (1984) summarized weathering data for a variety of silicates at pH 5. The specific oxidation rates of metacinnabar measured here, under similar pH conditions, are among the slowest weathering of these minerals, with a weathering rate in the same range as minerals such as quartz and K-feldspar which are considered environmentally stable in soils (Drever, 1988).

### 3.3. Adsorption experiments

Both batch and column oxidation experiments indicated the dissolved Hg(II) production rate was much lower than the dissolution rate. Based on these results and those of Burkstaller et al. (1975), it was hypothesized that the Hg released during dissolution was being adsorbed to the metacinnabar surface. To test this hypothesis, batch experiments were conducted to measure

the extent of adsorption of dissolved Hg(II) to metacinnabar, and the results were fit to several conventional, non-electrostatic adsorption isotherms. The data were best described by a Freundlich isotherm

$$q = K_f C^n \quad (7)$$

where  $q$  is the amount of Hg(II) adsorbed per unit mass of metacinnabar ( $\mu\text{g}/\text{g}$ ),  $C$  is the aqueous concentration of Hg(II) at equilibrium ( $\mu\text{g}/\text{ml}$ ) and  $K_f$  and  $n$  are constants (Fig. 4). Experimentally determined values of  $q$  and  $C$  were used to fit Eq. (7) using non-linear, least-squares regression assuming constant absolute error. The fitted values of  $K_f$  and  $n$  were  $659 (\pm 20)$  and  $0.153 (\pm 0.009)$  respectively; the solid curve shown in Fig. 4 is calculated from Eq. (7) and the fitted constants. The results confirmed that Hg(II) is strongly adsorbed to metacinnabar; the isotherm is highly non-linear, with a very large slope at low solute concentrations. This type of isotherm indicates a high degree of affinity between Hg(II) and metacinnabar, which is characteristic of specific adsorption (Sposito, 1984).

### 3.4. Mercury release rate

The results above indicate that metacinnabar, under the conditions described above, weathers slowly in comparison to other minerals normally considered stable in soils such as quartz and K-feldspar. Further, the Hg release rate is much lower than the dissolution rate due to the adsorption of the released Hg to the remaining metacinnabar surface. These experiments, however, used very high metacinnabar/solution ratios in order to produce  $\text{SO}_4^{2-}$  concentrations high enough to be measured from which the dissolution rate could be calculated. However, high metacinnabar/solution ratios also favor lower Hg release rates because of the larger surface area available for Hg adsorption. In order to

Table 4  
Comparison of mineral dissolution rates

Mineral	Conditions	Rate <sup>a</sup> $\mu\text{mol}/\text{m}^2/\text{day}$ ( $\mu\text{mol}/\text{g}/\text{day}$ )
Metacinnabar ( $\beta\text{-HgS}$ )	pH 4.7, $\text{O}_2$ , $T = 23^\circ\text{C}$ , $I = 0.01 \text{ M}$	$1.34 \times 10^{-2}$ – $5.87 \times 10^{-2}$ ( $1.31 \times 10^{-2}$ – $5.75 \times 10^{-2}$ )
Quartz <sup>b</sup> ( $\text{SiO}_2$ )	pH 5, $T = 25^\circ\text{C}$	$3.5 \times 10^{-3}$
K-Feldspar <sup>b</sup> ( $\text{KAlSi}_3\text{O}_8$ )	pH 5, $T = 25^\circ\text{C}$	$4.8 \times 10^{-2}$
Albite <sup>b</sup> ( $\text{NaAlSi}_3\text{O}_8$ )	pH 5, $T = 25^\circ\text{C}$	$3.4 \times 10^{-1}$
Pyrite <sup>c</sup> ( $\text{FeS}_2$ )	pH 6.7–8.5, $T = 23$ – $25^\circ\text{C}$ , $I = 0.005 \text{ M}$	(0.58–2.3)
Cinnabar <sup>d</sup> ( $\alpha\text{-HgS}$ )	pH 1.5, 10 mM Fe(III), $T = 25^\circ\text{C}$ , $I = 0.067 \text{ M}$	(0.7–8)

<sup>a</sup> Rates reported in units of  $\mu\text{mol}/\text{m}^2/\text{day}$  where available. Rates in parentheses are in units of  $\mu\text{mol}/\text{g}/\text{day}$ .

<sup>b</sup> Summarized in Lasaga (1984).

<sup>c</sup> Nicholson et al. (1988).

<sup>d</sup> Burkstaller et al. (1975).

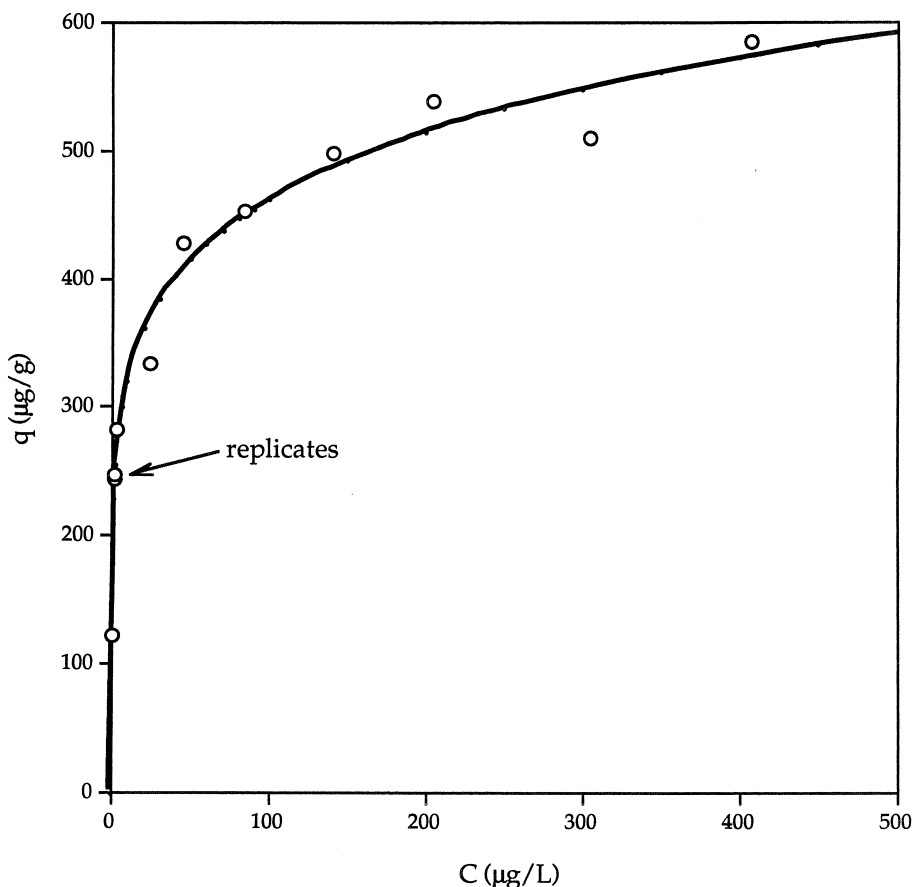


Fig. 4. Equilibrium batch isotherm for Hg(II) on metacinnabar at pH 4 ( $I=0.01$  M,  $T=23^{\circ}\text{C}$ ), where  $q$  is the amount of Hg(II) adsorbed per unit mass of metacinnabar ( $\mu\text{g/g}$ ) and  $C$  is the aqueous concentration of Hg(II) at equilibrium ( $\mu\text{g/l}$ ). Error bars based on one set of triplicate samples (shown on the diagram) are smaller than the data points. Solid curve is calculated from the Freundlich isotherm and fitted constants (see text).

better investigate the Hg release rate during dissolution, a second column with a lower solid phase metacinnabar concentration was also utilized (Experiments D–G, Table 1). This column contained 2000 mg/kg of HgS, which was designed to replicate the subsurface conditions at EFPC, a Hg-contaminated site where metacinnabar has formed (Barnett et al., 1997). Eluent solutions containing 0.01 M NaCl, pH adjusted from 5 to 9 to encompass the pH range of most natural waters, a low-DOC natural surface water (WOC, Table 2) and a high DOC natural surface water (EVG, Table 2) were also used to investigate the effects of a wider range of chemical composition on the Hg release rate.

Decreasing the HgS concentration in the solid phase resulted in an increase in the Hg release rate. This inverse relationship between HgS solid-solution ratio and Hg release rate is consistent with the relationship observed by Burkstaller et al. (1975). The total effluent Hg concentrations in 0.01 M NaCl (Experiment D, Table 1) ranged from 30 to 610 pM with

an average concentration of 240 pM (Fig. 5). Although the pH was varied, there was no systematic relationship between pH and Hg concentration (Fig. 5). The Hg release rate based on these effluent Hg concentrations ranged from  $6.97 \times 10^{-5}$  to  $1.42 \times 10^{-3}$   $\mu\text{mol/m}^2/\text{day}$  ( $I=0.01$  M,  $23^{\circ}\text{C}$ ), which was more than one order of magnitude less than the total weathering rates measured above.

Recent research has shown that DOC may play an important role in the formation and weathering of HgS in the environment (Ravichandran et al., 1998,1999), and the two DOC-containing natural waters did increase effluent Hg concentrations (Fig. 5) and the corresponding Hg release rate at a constant flow rate. The effluent Hg concentration when using low-DOC water (Experiment E, Table 1) as the eluent ranged from 850 to 1500 pM with an average of 1300 pM, which corresponds to a range in Hg release rates of  $1.97\text{--}3.62 \times 10^{-3}$   $\mu\text{mol/m}^2/\text{day}$  ( $I=0.01$  M,  $23^{\circ}\text{C}$ ). An increase in DOC concentration with the Everglades water (Experiment F,

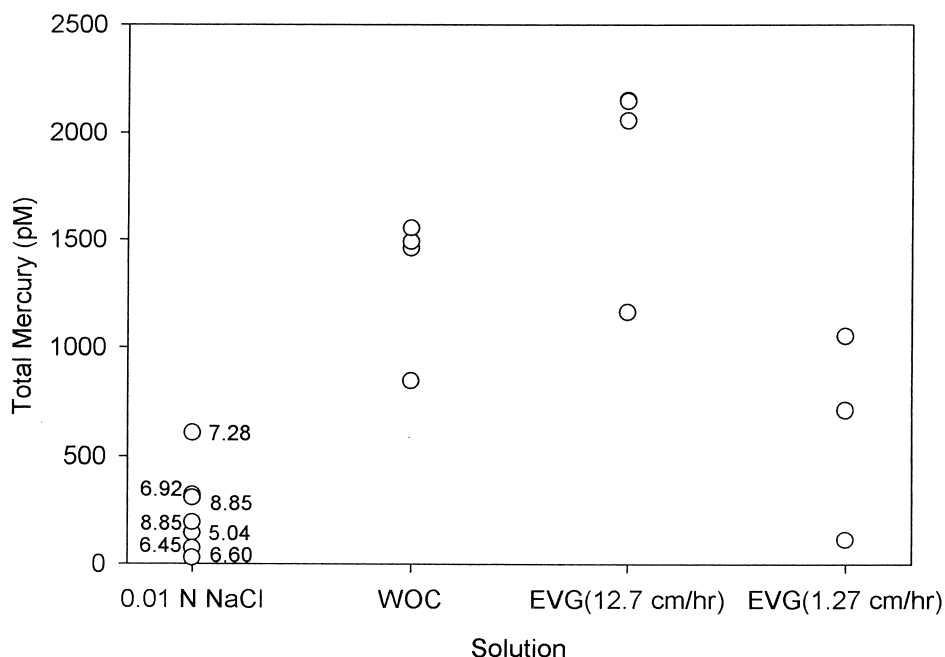


Fig. 5. Mercury concentrations in effluent from column 2. Effluent pH values are shown for Experiment D.

Table 1) resulted in an increase in Hg concentration from 1200 to 2100 pM, which corresponds to a range in Hg release rates of  $2.71\text{--}5.02 \times 10^{-3} \mu\text{mol}/\text{m}^2/\text{day}$  ( $I=0.01 \text{ M}$ ,  $23^\circ\text{C}$ ), approximately one order of magnitude lower than the dissolution rates measured above of  $1.34\text{--}5.87 \times 10^{-2} \mu\text{mol}/\text{m}^2/\text{day}$  ( $I=0.01 \text{ M}$ ,  $23^\circ\text{C}$ ).

In order to examine the effect of flow rate on the Hg release rate, the specific discharge was decreased by an order of magnitude to 1.27 cm/h (Experiment G, Table 1) while using the Everglades water as eluent. Decreasing the flow rate in the column resulted in a decrease in the effluent Hg concentration to 710–1100 pM and a decrease in the Hg release rate to  $2.67 \times 10^{-5}\text{--}2.45 \times 10^{-4} \mu\text{mol}/\text{m}^2/\text{day}$  ( $I=0.01 \text{ M}$ ,  $23^\circ\text{C}$ ). Decreasing the flow rate increased the solid/liquid contact time, which could result in both higher (Hg from oxidation) and lower (Hg lost due to adsorption) effluent Hg concentrations. The decrease in effluent Hg concentration with flow rate indicates the latter process is more important. Effluent  $\text{SO}_4^{2-}$  concentrations were below the detection limit for Experiments D–G, so dissolution rates could not be quantified.

The effluent Hg concentrations reported above are consistent with the results of Ravichandran et al. (1998, 1999). These authors reported that DOC isolated from natural waters enhanced HgS (cinnabar) dissolution but that natural waters containing DOC had no measurable effect on HgS dissolution. Ravichandran et al. (1998,1999) did not report any detectable Hg release (at

a detection limit of 2500 pM) from HgS using natural waters from the Everglades with similar DOC concentrations. In this work, Hg was detected in experiments involving Everglades water but at levels below Ravichandran's limit of detection (Fig. 5). Thus the results obtained in this work are consistent with Ravichandran's results. These effluent Hg concentrations are also within the same range or just above the groundwater concentrations at EFPC. EFPC is a Hg-contaminated floodplain where metacinnabar has formed (Barnett et al., 1997). Solid-phase Hg concentrations up to 3000 mg/kg and groundwater DOC concentrations of approximately 20 mg/l resulted in concentrations of dissolved Hg below or slightly above the minimum detectable concentration of 1000 pM used during the remedial investigation of the site.

These results reported above are not consistent with those of Hsieh et al. (1991). In contrast to this study, Hsieh et al. (1991) used low solid-solution ratios and thus were unable to detect any S products to quantify the total dissolution rate. Although the effective dissolution rates calculated on the basis of total Hg production were several times lower than the total dissolution rates measured in this investigation, these investigators reported significant amounts of dissolved Hg (up to approximately 0.2  $\mu\text{M}$ ) in their dissolution experiments. The reason for this discrepancy is unclear, but the authors were unable to replicate their results under the same experimental conditions (results not shown).

#### 4. Conclusions

The dissolution rate of metacinnabar by dissolved O<sub>2</sub> at pH ~5 measured in this investigation ranged from 1.34 (±0.11) to 5.87 (±0.39) × 10<sup>-2</sup> μmol/m<sup>2</sup>/day (I=0.01 M, 23°C) and was dependent on the hydrodynamic conditions. Although this range in rates is not large compared to the typical order of magnitude uncertainty in mineral weathering rates measured in the laboratory (Brezonik, 1994), the rates did increase significantly in more turbulent hydrodynamic conditions. These results were contrary to the published literature, theoretical calculations, and a measured activation energy of 77 (±8) kJ/mol (I=0.01 M). Thus it is possible the reaction may have been under mixed transport- and surface-control, or that some other physical process, such as a change in the effective wetted surface area, may have mimicked transport control. In either case, reaction rates in the field may be dependent on the prevailing hydrodynamic conditions.

The range of weathering rates reported here was slow compared to other minerals considered stable in the subsurface (e.g. quartz and K feldspar). In addition, the rate of Hg release under a range of hydrogeochemical conditions that more closely approximated those found in the subsurface (e.g. in porous media, in the presence of DOC, etc.) was 1 to 3 orders of magnitude lower than the dissolution rate, which was consistent with the adsorption of the Hg(II) released during weathering to the metacinnabar surface in exchange for two H<sup>+</sup> ions. These data were also consistent with the relatively low dissolved Hg concentrations observed at a Hg-contaminated site where metacinnabar had formed.

These results indicate that metacinnabar has the potential to serve as a long-term repository for Hg in the subsurface. The weathering rate of HgS in the environment may be influenced by additional factors not investigated in this research including the presence of solid phase Fe and Mn oxyhydroxides and sulfide-oxidizing microorganisms. The influence of these additional variables bears further investigation.

#### Acknowledgements

We are grateful to Phil Jardine and Steve Lindberg for their help and the use of their laboratories. M.O.B. was supported through an appointment to the US Department of Energy Laboratory Cooperative Post-graduate Research Training Program at Oak Ridge National Laboratory administered by the Oak Ridge Institute for Science and Education. This research was sponsored by the Environmental Restoration Division, US Department of Energy. Oak Ridge National Laboratory is managed by Lockheed Martin Energy Research Corp. for the US Department of Energy under contract number DE-AC05-96OR22464.

#### References

- Adriano, D.C., 1986. Trace Elements in the Terrestrial Environment. Springer-Verlag, New York.
- Appelo, C.A.J., Postma, D., 1993. Geochemistry, Groundwater and Pollution. A.A. Balkema, Rotterdam, Netherlands.
- ASTM, 1991. Annual Book of ASTM Standards. American Society for Testing and Materials, Philadelphia, PA.
- Azzaria, L.M., Aftabi, A., 1991. Stepwise thermal analysis technique for estimating mercury phases in soils and sediments. Water, Air Soil Pollut. 56, 203–217.
- Barnett, M.O., Harris, L.A., Turner, R.R., Stevenson, R.J., Henson, T.J., Melton, R.C., Hoffman, D.P., 1997. Formation of mercuric sulfide in soil. Environ. Sci. Technol. 31, 3037–3043.
- Brezonik, P.L., 1994. Chemical Kinetics and Process Dynamics in Aquatic Systems. Lewis Publishers, Ann Arbor, MI.
- Burkstaller, J.E., McCarty, P.L., Parks, G.A., 1975. Oxidation of cinnabar by Fe(III) in acid mine waters. Environ. Sci. Technol. 9, 676–678.
- Drever, J.I., 1988. The Geochemistry of Natural Waters. Prentice Hall, Englewood Cliffs, NJ.
- EPA, 1986. SW-846: Test Methods for Evaluating Solid Waste: Physical/Chemical Methods. US Environmental Protection Agency, Washington, DC.
- EPA, 1995. Method 1631: Mercury in Water by Oxidation, Purge and Trap, and Cold Vapor Atomic Fluorescence Spectrometry (Draft). US Environmental Protection Agency, Washington, DC.
- Fitzgerald, W.F., Engstrom, D.R., Mason, R.P., Nater, E.A., 1998. The case for atmospheric mercury contamination in remote areas. Environ. Sci. Technol. 32, 1–7.
- Hoffman, M.R., 1977. Kinetics and mechanisms of oxidation of hydrogen sulfide by hydrogen peroxide in acidic solution. Environ. Sci. Technol. 11, 61–66.
- Hsieh, Y.H., Tokunaga, S., Huang, C.P., 1991. Some chemical reactions at the HgS(s)-water interface as affected by photoirradiation. Colloids and Surfaces 53, 257–274.
- Hurley, J.P., Krabbenhoft, D.P., Babiarz, C.L., Andren, A.W., 1994. Cycling of Mercury across the Sediment-Water Interface in Seepage Lakes. In: Baker, L.A. (Ed.), Environmental Chemistry of Lakes and Reservoirs. American Chemical Society, Washington, DC, pp. 425–450.
- Kaiser, G., Tolg, G., 1980. Mercury. In: Hutzinger, O. (Ed.), The Handbook of Environmental Chemistry, Volume 3, Part A, Anthropogenic Compounds. Springer-Verlag, New York, pp. 1–58.
- Krabbenhoft, D.P., Babiarz, C.L., 1992. The role of ground-water transport in aquatic mercury cycling. Water Resour. Res. 28, 3119–3128.
- Lasaga, A.C., 1984. Chemical kinetics of water-rock interactions. J. Geophys. Res. 89, 4009–4025.
- Lechler, P.J., Miller, J.R., Hsu, L.C., Desilets, M.O., 1997. Mercury mobility at the Carson River Superfund Site, west-central Nevada, USA: interpretation of mercury speciation data in mill tailings, soils, and sediments. J. Geochem. Explor. 58, 259–267.
- McKibben, M.A., Barnes, H.L., 1986. Oxidation of pyrite in low temperature acidic solutions: rate laws and surface textures. Geochim. Cosmochim. Acta 50, 1509–1520.
- Moses, C.O., Nordstrom, D.K., Herman, J.S., Mills, A.L.,

1987. Aqueous pyrite oxidation by dissolved oxygen and by ferric iron. *Geochim. Cosmochim. Acta* 51, 1561–1571.
- Nicholson, R.V., Gillham, R.W., Reardon, E.J., 1988. Pyrite oxidation in carbonate buffered solution: 1. Experimental kinetics. *Geochim. Cosmochim. Acta* 52, 1077–1085.
- Nicholson, R.V., Gillham, R.W., Reardon, E.J., 1990. Pyrite oxidation in carbonate-buffered solution: 2. Rate control by oxide coatings. *Geochim. Cosmochim. Acta* 54, 395–402.
- Nielsen, A.E., 1964. *Kinetics of Precipitation*. MacMillan, New York.
- Okouchi, S., Sasaki, S., 1983. Photochemical behavior of mercury ore in water. *Environ. Internat.* 9, 103–106.
- Paquette, K.A., Helz, G.R., 1997. Inorganic speciation of mercury in sulfidic waters: the importance of zero-valent sulfur. *Environ. Sci. Technol.* 31, 2148–2153.
- Plouffe, A., 1997. Physical partitioning of mercury in till: an example from central British Columbia, Canada. *J. Geochem. Explor.* 59, 219–232.
- Ravichandran, M., Aiken, G.R., Reddy, M.M., Ryan, J.N., 1998. Enhanced dissolution of cinnabar (mercuric sulfide) by dissolved organic matter from the Florida Everglades. *Environ. Sci. Technol.* 32, 3305–3311.
- Ravichandran, M., Aiken, G.R., Ryan, J.N., Reddy, M.M., 1999. Inhibition of precipitation and aggregation of meta-cinnabar (mercuric sulfide) by dissolved organic matter isolated from the Florida Everglades. *Environ. Sci. Technol.* 33, 1418–1423.
- Ronngren, L., Sjoberg, S., Sun, Z., Forsling, W., Schindler, P.W., 1991. Surface reactions in aqueous metal sulfide systems. 2. Ion exchange and acid/base reactions at the ZnS–H<sub>2</sub>O Interface. *J. Colloid Interface Sci.* 145, 396–404.
- Sakamoto, H., Tomiyasu, T., Yonehara, N., 1995. The contents and chemical forms of mercury in sediments from Kagoshima Bay, in comparison with Minamata Bay and Yatsushiro, southwestern Japan. *Geochem. J.* 29, 97–105.
- Satake, K., Shibata, K., Bando, Y., 1990. Mercury sulphide (HgS) crystals in the cell walls of the aquatic bryophytes, *Jungermannia vulcanicola* Steph. and *Scapania undulata* (L.). *Dum. Aquat. Bot.* 36, 325–341.
- Sposito, G., 1984. *The Surface Chemistry of Soils*. Oxford University Press, New York.
- Stein, E.D., Cohen, Y., Winer, A.M., 1996. Environmental distribution and transformation of mercury compounds. *Crit. Rev. Environ. Sci. Technol.* 26, 1–43.
- Stumm, W., 1992. *Chemistry of the Solid-Water Interface*. John Wiley & Sons, New York.
- Tauson, V.L., Akimov, V.V., 1997. Introduction to the theory of forced equilibria: general principles, basic concepts and definitions. *Geochim. Cosmochim. Acta* 61, 4935–4944.
- Thibodeaux, L.J., 1996. *Environmental Chemodynamics*. John Wiley & Sons, New York.
- Wang, W., Driscoll, C.T., 1995. Patterns of total mercury concentrations in Onondaga Lake, New York. *Environ. Sci. Technol.* 29, 2261–2266.
- Willet, K.L., Turner, R.R., Beauchamp, J.J., 1992. Effect of chemical form of mercury on the performance of dosed soils in standard leaching protocols: EP and TCLP. *Hazard. Waste Hazard. Mater.* 9, 275–288.